Uncoupling of Obesity from Insulin Resistance Through a Targeted Mutation in *aP2*, the Adipocyte Fatty Acid Binding Protein

Gökhan S. Hotamisligil,* Randall S. Johnson, Robert J. Distel, Ramsey Ellis, Virginia E. Papaioannou, Bruce M. Spiegelman*

Fatty acid binding proteins (FABPs) are small cytoplasmic proteins that are expressed in a highly tissue-specific manner and bind to fatty acids such as oleic and retinoic acid. Mice with a null mutation in *aP2*, the gene encoding the adipocyte FABP, were developmentally and metabolically normal. The *aP2*-deficient mice developed dietary obesity but, unlike control mice, they did not develop insulin resistance or diabetes. Also unlike their obese wild-type counterparts, obese $aP2^{-/-}$ animals failed to express in adipose tissue tumor necrosis factor–α (TNF-α), a molecule implicated in obesity-related insulin resistance. These results indicate that *aP2* is central to the pathway that links obesity to insulin resistance, possibly by linking fatty acid metabolism to expression of TNF-α.

Fatty acids are important metabolic fuels and may also function as physiological signaling molecules. To investigate the functional role of the adipocyte FABP in fatty acid action, we created a null mutation in the *aP2* gene by homologous recombination, as described (*1*). Germline transmission of the targeted allele was followed by back-crossing between six to eight generations onto C57Bl6/J mice and sib crosses to obtain homozygous null mice on an inbred background (*2*). The complete absence of *aP2* mRNA expression in adipose tissues of the homozygous *aP2* mutant (−/−) mice was confirmed by Northern (RNA) blot (Fig. 1A) and reverse transcription polymerase chain reaction analysis (*3*), both of which revealed no expression of *aP2* mRNA. The aP2 protein was also undetectable in adipose tissue by protein immunoblot analysis (Fig. 1B). Under standard laboratory conditions, the $aP2^{-/-}$ mice did not differ from their wild-type ($aP2^{+/+}$) and heterozygous ($aP2^{+/-}$) littermates in breeding, behavior, or development. Morphologically, adipose tissue appeared normal. Most of the genes specifically expressed in adipose tissue that were examined exhibited no obvious differences in mRNA expression patterns in the $aP2^{-/-}$ mice (Fig. 1C). Growth curves, body weight, and body composition, as well as glucose and lipid metabolism, were also similar between the $aP2^{-/-}$, $aP2^{+/-}$, and $aP2^{+/+}$ animals. There was a small decrease in the amount of circulating triglyceride in $aP2^{-/-}$ mice (Table 1).

This lack of an obvious morphological or metabolic phenotype in the *aP2*-deficient mice raised the possibility of redundancy in fatty acid (FA) binding capacity in adipose tissue. Of the other FABP mRNAs examined (*4*), only that for keratinocyte FABP (*mal1*) was detected in fat tissue (Fig. 1D) (*5*). Small amounts of *mal1* expression were evident in the adipose tissues of $aP2^{+/+}$ animals, and larger amounts were present in both $aP2^{+/-}$ (≈4-fold increase) and $aP2^{-/-}$ (≈20-fold increase) animals (Fig. 1D). The amount of MAL1 protein was also increased in adipose tissue of $aP2^{-/-}$ mice (*6*). These results indicate that the $aP2^{-/-}$ animals may maintain a relatively normal physiology through a compensatory increase in expression of MAL1.

To test whether low amounts of FAs in normal diets of these mice in the lab (*7*) might obscure the biological role of aP2, we placed the *aP2*-deficient mice on a high-fat (40% of the total calories in the form of fat) and high-caloric (3490 kcal per kilogram of body weight) diet. On this diet, both the $aP2^{+/+}$ and $aP2^{-/-}$ mice developed obesity, although the total weight gain in the $aP2^{-/-}$ animals was higher than that of the $aP2^{+/+}$ animals (Fig. 1E). This is likely to be the result of increased adiposity because preliminary experiments showed that the epididymal fat pad weight in the $aP2^{-/-}$ mice was higher than that of the $aP2^{+/+}$ animals (*8*). The obese *aP2*-deficient mice had marginally higher plasma free fatty acids (FFAs) but lower triglyceride levels (Table 1), indicating that the lack of aP2 did not negatively affect the FA uptake by adipose tissue but potentially interfered with triglyceride synthesis or secretion, or both.

We next investigated glucose homeostasis in wild-type and *aP2*-deficient animals rendered obese by the high-fat diet. Obese $aP2^{+/+}$ and $aP2^{+/-}$ mice developed hyperinsulinemia (5.9 ± 0.9 and 2.7 ± 0.4 ng/ml, respectively), which is usually taken as a compensatory response to the development of obesity-induced insulin resistance (Fig. 2A) (*7*). In contrast, insulin concentrations in obese *aP2*-deficient animals were lower (0.7 ± 0.2 ng/ml, $P < 0.01$) than those in wild-type and heterozygous mice (Fig. 2A) and were indistinguishable from those in lean $aP2^{+/+}$, $aP2^{+/-}$, and $aP2^{-/-}$ mice (0.87 ± 0.07, 0.75 ± 0.05, and 0.8

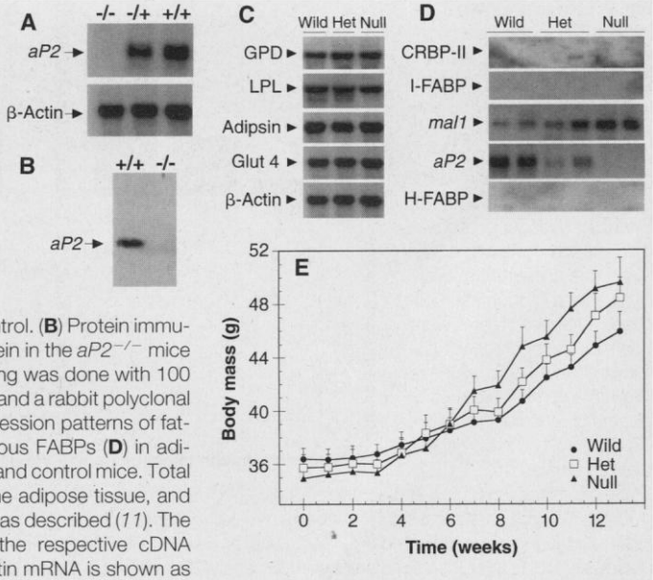

Fig. 1. Generation of *aP2*-deficient mice. (**A**) Northern blot analysis of *aP2* mRNA in the fat tissues of the $aP2^{-/-}$ mice and controls. Total RNA was extracted from adipose tissue, and 10 μg was used for blotting, as described (*11*). The blots were hybridized to the mouse *aP2* cDNA probe as described (*11*). β-Actin mRNA is shown as a control. (**B**) Protein immunoblot analysis of AP2 protein in the $aP2^{-/-}$ mice and controls. Immunoblotting was done with 100 μg of total fat tissue extract and a rabbit polyclonal antibody against AP2. Expression patterns of fat-specific genes (**C**) and various FABPs (**D**) in adipose tissues of the $aP2^{-/-}$ and control mice. Total RNA was extracted from the adipose tissue, and 10 μg was used for blotting as described (*11*). The blots were hybridized to the respective cDNA probes as described. β-Actin mRNA is shown as a control. (**E**) Growth curves of $aP2^{-/-}$, $aP2^{+/-}$, and $aP2^{+/+}$ mice fed a high-fat–containing diet (Research Diets). Body mass (g) is provided as the mean ± SEM.

G. S. Hotamisligil, Department of Nutrition, Harvard School of Public Health, 665 Huntington Avenue, Boston, MA 02115, USA.
R. S. Johnson, Department of Biology, University of California, San Diego, La Jolla, CA 92093, USA.
R. J. Distel, R. Ellis, B. M. Spiegelman, Dana Farber Cancer Institute and Department of Cell Biology, Harvard Medical School, Boston, MA 02115, USA.
V. E. Papaioannou, Department of Genetics and Development, Columbia University, 701 West 168 Street, New York, NY 10032, USA.
*To whom correspondence should be addressed.

± 0.03 ng/ml, respectively). Despite much greater circulating amounts of insulin, the wild-type mice had higher blood glucose concentrations (230 ± 25 mg/dl) than the $aP2^{-/-}$ animals (150 ± 17 mg/dl) (Fig. 2B). These results indicate that the absence of *aP2* interferes with the development of dietary obesity-induced insulin resistance.

To more directly address this possibility, we performed intraperitoneal insulin (IITT) and glucose (IGTT) tolerance tests on these mice. The hypoglycemic response to insulin was less in the obese $aP2^{+/+}$ and $aP2^{+/-}$ mice at 15 to 60 min than that in obese $aP2^{-/-}$ animals (Fig. 2C). IGTT also revealed higher amounts of hyperglycemia in the obese $aP2^{+/+}$ and $aP2^{+/-}$ animals after 15 to 60 min than that in obese $aP2^{-/-}$ mice (Fig. 2D). Thus, both of these tests revealed insulin resistance in obese $aP2^{+/+}$ and $aP2^{+/-}$ animals but not in obese $aP2^{-/-}$ mice. These mice provide an animal model in which obesity can be genetically uncoupled from insulin resistance.

Several genes expressed in adipose tissue, such as *TNF*-α and *ob*, are implicated in insulin resistance (*9*, *10*). Overexpression of TNF-α in fat tissue occurs in virtually all models of obesity and insulin resistance examined to date (*11*, *12*). TNF-α inhibits the insulin-stimulated tyrosine kinase activity of the insulin receptor, in vitro and in vivo (*13*). TNF-α also down-regulates expression of the insulin-sensitive glucose transporter (Glut4) (*14*). *TNF*-α expression in the adipose tissues of obese $aP2^{-/-}$ mice was lower than that in the obese $aP2^{+/-}$ or $aP2^{+/+}$ animals (Fig. 3A). However, $aP2^{-/-}$ mice appear not to have an intrinsic deficiency in regulation of the *TNF*-α gene. When stimulated with bacterial lipopolysaccharide (LPS), $aP2^{-/-}$ animals, like wild-type controls, expressed large amounts of *TNF*-α mRNA in their adipose tissues (Fig. 3B). No *TNF*-α mRNA was detectable in the lean animals of any of the genotypes. Expression of the *ob* gene, another fat-specific gene that has been suggested to affect insulin sensitivity, was not significantly different among the different genotypes (Fig. 3A). Thus, the lack of insulin resistance in obese $aP2^{-/-}$ mice was specifically correlated with lack of obesity-induced *TNF*-α expression in adipose tissue. The failure to regulate *TNF*-α might contribute to the uncoupling of obesity and insulin resistance in the $aP2^{-/-}$ mice.

In obesity, insulin resistance appears to occur in all of the major insulin-sensitive tissues: fat, muscle, and liver (*15*). Because *aP2* is expressed exclusively in adipocytes, our results demonstrate an active role for adipocytes and adipose tissue in abnormal glucose homeostasis in obesity. However, the range of insulin-sensitive tissues that are affected by the absence of *aP2* remains to be determined.

This study provides further evidence that FAs participate in the pathway that induces insulin resistance (*16*). Obese individuals often have increased amounts of FFAs and triglycerides in addition to insulin resistance. Furthermore, feeding high-fat diets to rodents induces insulin resistance that is dependent on both the dose and the specific types of FAs included in the diet (*7*). Administration of FFAs to normal individuals induces a mild state of insulin

Table 1. Comparison of biochemical parameters in lean and obese $aP2^{-/-}$, $aP2^{+/-}$, and $aP2^{+/+}$ mice. Plasma insulin and glucose were measured after an overnight fast as described in Fig. 2. Plasma lipids were measured as described (*13*). The experiments were duplicated in two consecutive generations. Each value is the mean ± SEM of measurements on at least 10 mice. Mean values of each plasma component are compared between $aP2^{-/-}$ mice and wild-type controls by Student's *t* test (*P = 0.05 and **$P \leq 0.005$).

Parameter	Wild type ($aP2^{+/+}$)		Heterozygote ($aP2^{+/-}$)		Null ($aP2^{-/-}$)	
	Lean	Obese	Lean	Obese	Lean	Obese
Insulin (ng/ml)	0.87 ± 0.07	5.9 ± 0.9	0.75 ± 0.05	2.7 ± 0.46	0.80 ± 0.03	0.75 ± 0.2**
Glucose (mg/dl)	140 ± 18	230 ± 25	130 ± 11	200 ± 18	139 ± 7.5	150 ± 17*
FFA (mM)	0.36 ± 0.06	0.47 ± 0.05	0.39 ± 0.04	0.49 ± 0.04	0.44 ± 0.04	0.51 ± 0.04
Triglyceride (mg/dl)	104 ± 10	123 ± 15	87 ± 7	100 ± 11	76 ± 5*	81.1 ± 9.3*
Cholesterol (mg/dl)	111 ± 10.6	121 ± 21	108 ± 14	118 ± 15	105 ± 9.5	125 ± 13

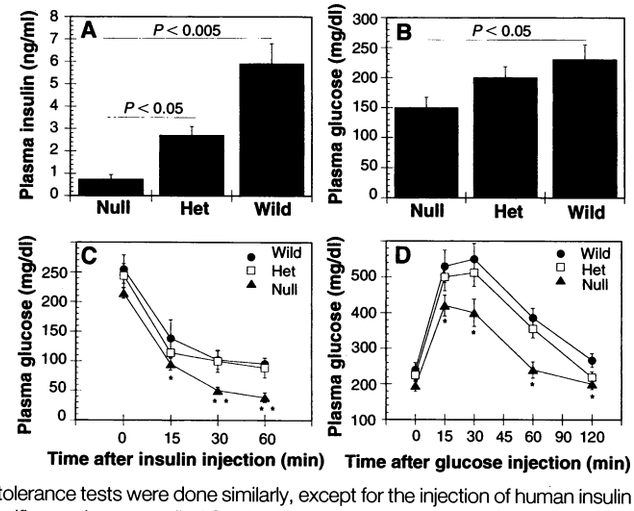

Fig. 2. Glucose homeostasis in the $aP2^{-/-}$ mice and controls during fasting. (**A**) Glucose and (**B**) insulin concentrations in plasma were measured after an overnight fast with a Beckman automated glucose analyzer and a radioimmunoassay (Linco, St. Charles, Missouri), respectively. (**C**) Glucose and (**D**) insulin tolerance tests were done after a 6-hour fast. Glucose tolerance tests were done by intraperitoneal administration of glucose (3 g/kg) and measurement of plasma glucose at t = 0, 15, 30, 60, and 120 min in anesthetized male, 12- to 13-week-old mice ($n \geq 8$). Insulin tolerance tests were done similarly, except for the injection of human insulin (1 IU/kg) (Eli Lilly). Statistical significance in a two-tailed Student's *t* test comparing $aP2^{-/-}$ and wild-type mice at a given time is indicated by * ($P < 0.05$) and ** ($P < 0.005$). Investigation of the dynamics of the responses to the tolerance tests were done by analysis of variance repeated measures analysis (Statview 4.01, Abacus Concepts) and demonstrated statistically significant differences between $aP2^{-/-}$ mice and wild-type controls in both tests ($P < 0.001$).

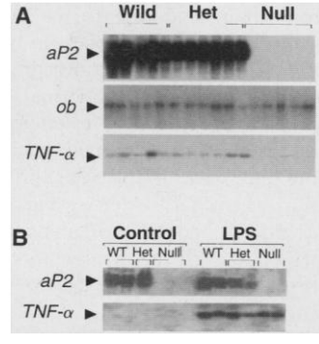

Fig. 3. *TNF*-α expression in adipose tissue from (**A**) obese $aP2^{-/-}$ mice and obese controls or (**B**) after LPS administration. Total RNA was extracted from the adipose tissue and 20 μg was used for blotting. The blots were hybridized to the mouse *ob*, *aP2*, or *TNF*-α cDNA probes as described (*11*). Lipopolysaccharide (1 mg/kg, Sigma) was injected intraperitoneally and tissues were collected 3 hours after the injection for RNA extraction and analysis.

resistance (*16*). Treatment of cultured cells with FFAs suppresses insulin action at the level of the insulin receptor (*16*). However, the specific mechanisms by which FFAs induce insulin resistance are not understood. Our results suggest that FFAs might induce insulin resistance by increasing the expression of *TNF*-α or other genes that interfere with insulin action. aP2 might play a role in regulation of gene expression by binding and shuttling these FFAs to the target cellular compartments.

REFERENCES AND NOTES

1. R. S. Johnson *et al.*, *Science* **245**, 1234 (1989).
2. V. E. Papaioannou and R. S. Johnson, in *Gene Targeting: A Practical Approach*, A. L. Joyner, Ed. (IRL, Oxford, 1993), pp. 107–146.
3. G. S. Hotamisligil, unpublished observations.
4. V. Matarese, R. L. Stone, D. W. Waggoner, D. A. Bernlohr, *Prog. Lipid Res.* **28**, 245 (1989).
5. P. Krieg, S. Feil, G. Fürstenberger, G. T. Bowden, *J. Biol. Chem.* **268**, 17362 (1993).
6. D. A. Bernlohr, unpublished observations.
7. D. Lemonnier, J. P. Suquet, R. Aubert, P. De Gasquet, E. Pequignot, *Diabetes Metab. (Paris)* **1**, 77 (1975); D. M. W. Salmon and J. P. Flatt, *Int. J. Obesity* **9**, 443 (1985); L. H. Storlien *et al.*, *Diabetes* **40**, 280 (1990).
8. J. Storch and S. Fried, unpublished observations.
9. G. S. Hotamisligil and B. M. Spiegelman, *Diabetes* **43**, 1271 (1994).
10. J. L. Halaas *et al.*, *Science* **269**, 543 (1995); M. A. Pelleymounter *et al.*, *ibid.*, p. 540; L. A. Campfield, F. J. Smith, Y. Guisez, R. Devos, P. Burn, *ibid.*, p. 546.
11. G. S. Hotamisligil, N. S. Shargill, B. M. Spiegelman, *ibid.* **259**, 87 (1993); C. Hofmann *et al.*, *Endocrinology* **134**, 264 (1994); A. Hamann *et al.*, *Diabetes* **44**, 1266 (1995).
12. G. S. Hotamisligil, P. Arner, J. F. Caro, R. L. Atkinson, B. M. Spiegelman, *J. Clin. Invest.* **95**, 2409 (1995); P. A. Kern *et al.*, *ibid.*, p. 2111.
13. G. S. Hotamisligil, D. L. Murray, L. N. Choy, B. M. Spiegelman, *Proc. Natl. Acad. Sci. U.S.A.* **91**, 4854 (1994); R. Feinstein, H. Kanety, M. Z. Papa, B. Lunenfeld, A. Karasik, *J. Biol. Chem.* **268**, 26055 (1993); G. S. Hotamisligil, A. Budavari, D. L. Murray, B. M. Spiegelman, *J. Clin. Invest.* **94**, 1543 (1994); G. H. Hotamisligil *et al.*, *Science* **271**, 665 (1996); H. Kanety, R. Feinstein, M. Z. Papa, R. Hemi, A. Karasik, *J. Biol. Chem.* **270**, 23780 (1995); G. Kroder *et al.*, *J. Clin. Invest.* **97**, 1471 (1996).
14. J. M. Stephens and P. H. Pekala, *J. Biol. Chem.* **266**, 21839 (1991).
15. D. E. Moller, *Insulin Resistance* (Wiley, West Sussex, UK, 1993).
16. P. J. Randle, P. B. Garland, L. N. Hales, E. A. Newsholme, *Lancet* **i**, 785 (1963); E. Ferrannini, E. J. Barret, S. Bevilacqua, R. A. De Fronzo, *J. Clin. Invest.* **72**, 1737 (1983); J. Svedberg, P. Bjorntorp, U. Smith, P. Lonnroth, *Diabetes* **39**, 570 (1990).

17. We thank J. Storch, S. Fried, and D. Bernlohr for sharing unpublished observations, P. Krieg for the *mal1* cDNA, and J. Spencer and T. Uysal for technical help. Supported by funds from NIH grants DK31405 (B.M.S.) and HD27295 (V.E.P.) and the American Diabetes Association (G.S.H. and B.M.S.).

13 May 1996; accepted 20 September 1996

Liver Failure and Defective Hepatocyte Regeneration in Interleukin-6–Deficient Mice

Drew E. Cressman,* Linda E. Greenbaum, Robert A. DeAngelis, Gennaro Ciliberto, Emma E. Furth, Valeria Poli, Rebecca Taub†

Liver regeneration stimulated by a loss of liver mass leads to hepatocyte and nonparenchymal cell proliferation and rapid restoration of liver parenchyma. Mice with targeted disruption of the interleukin-6 (IL-6) gene had impaired liver regeneration characterized by liver necrosis and failure. There was a blunted DNA synthetic response in hepatocytes of these mice but not in nonparenchymal liver cells. Furthermore, there were discrete G_1 phase (prereplicative stage in the cell cycle) abnormalities including absence of STAT3 (signal transducer and activator of transcription protein 3) activation and depressed AP-1, Myc, and cyclin D1 expression. Treatment of IL-6–deficient mice with a single preoperative dose of IL-6 returned STAT3 binding, gene expression, and hepatocyte proliferation to near normal and prevented liver damage, establishing that IL-6 is a critical component of the regenerative response.

Because of the distinctive replication potential of adult hepatocytes, the liver has the ability to regenerate, allowing for rapid recovery after partial hepatectomy, liver transplant, or toxic injury (*1*, *2*). After a 70% partial hepatectomy, in which the two largest lobes of the liver are removed intact without injury to remnant liver cells, more than 95% of the mature, normally quiescent cells in the remnant liver rapidly proliferate, restoring liver mass in a few days. Answers to the central questions about liver regeneration remain elusive, including the identity of the initiating signals in regeneration and the mechanism by which liver cells continue to function while they are regenerating.

Two transcription factor complexes, nuclear factor kappa B (NF-κB) and STAT3, are rapidly activated by means of posttranslational modifications in the remnant liver within minutes to hours after hepatectomy and may provide clues to the initiating signals (*3*, *4*). Epidermal growth factor (EGF), IL-6, and related cytokines are among the factors capable of stimulating STAT3 DNA binding activity in mouse liver nuclei (*5*). Because it is a hepatocyte mitogen (*1*, *2*), initially it appeared likely that EGF was responsible for induction of STAT3 after hepatectomy. However, a role for gut and Kupffer cell (liver macrophage)–derived cytokines, IL-1, IL-6, and tumor necrosis factor–α (TNF-α), was suggested to us in part because the transcription complexes NF-κB and STAT3 are both linked to cytokine activation pathways (*2*–*5*), an intact portal circulation is required for normal regeneration, and germ-free and lipopolysaccharide (LPS)–deficient animals show a blunted regenerative response (*6*). An in vitro study suggests a supportive role for IL-6 in hepatocyte proliferation (*7*), but, although controversial, most of the data suggest that large quantities of TNF-α may actually increase liver injury (*8*).

With the availability of mice harboring a targeted disruption of the gene encoding IL-6, we were able to determine whether IL-6 is responsible for activating STAT3 after hepatectomy. IL-6–deficient ($IL\text{-}6^{-/-}$) mice are developmentally normal and display abnormalities in the hepatic acute-phase response, some immune mechanisms, and bone resorption in response to estrogen (*9*–*11*). Antibody supershift experiments demonstrated that a STAT3 complex was induced in hepatectomized mouse livers (*12*) (Fig. 1A). STAT5, also a 92-kD protein, is activated in mouse liver in response to EGF stimulation (*13*); however, antibodies to STAT5 did not supershift the complex after hepatectomy. STAT3 DNA binding was strongly induced in the IL-6–containing ($IL\text{-}6^{+/+}$) remnant liver nuclear extracts with appearance 0.5 hour, peak activity 2 hours, and continued elevation 8 hours after hepatectomy (Fig. 1B), correlating well with results in rats (*4*). In $IL\text{-}6^{-/-}$ mice, STAT3 DNA binding was virtually absent, suggesting that STAT3 induction during liver regeneration is strictly mediated by IL-6. There was little induction of STAT3 binding after sham surgery in $IL\text{-}6^{+/+}$ animals and none in the $IL\text{-}6^{-/-}$ mice (Fig. 1C), confirming that STAT3 activation is specific to the regenerative response of the liver and not due to an acute-phase response induced by the surgical procedure.

D. E. Cressman, L. E. Greenbaum, R. A. DeAngelis, R. Taub, Department of Genetics and Medicine, University of Pennsylvania School of Medicine, 705a Stellar-Chance, 422 Curie Boulevard, Philadelphia, PA 19104–6145, USA.
G. Ciliberto and V. Poli, Instituto di Ricerche di Biologia Molecolare, IRBM Pietro Angeletti, Via Pontina Km 30.600, Pomezia (Roma), Italy.
E. E. Furth, Department of Pathology, University of Pennsylvania School of Medicine, 705a Stellar-Chance, 422 Curie Boulevard, Philadelphia, PA 19104–6145, USA.

*Present address: Duke University Medical Center, Research Drive, Durham, NC 27710, USA.
†To whom correspondence should be addressed.